American Mineralogist, Volume 66, pages 777–788, 1981

Enumeration of 4-connected 3-dimensional nets and classification of framework silicates: the infinite set of ABC-6 nets; the Archimedean and σ-related nets

JOSEPH V. SMITH

*Department of the Geophysical Sciences, University of Chicago
Chicago, Illinois 60637*

AND J. MICHAEL BENNETT

Union Carbide Corporation, Tarrytown, New York 10591

Abstract

Parallel 6-rings are linked by 4-rings into the infinite set of *ABC*-6 nets, and the 98 simplest nets are enumerated. These include the following types: afghanite, cancrinite, chabazite, erionite, gmelinite, levyne, liottite, losod, offretite, sodalite and TMA-E(AB). Unobserved species with fairly simple stacking and high symmetry include *AABC, AABCB, AABAB, AB CACB, AABBCCBB, AABCAACB, AABCBBAC, AABABBAB* and *ABCABACB*.

Nets with 4-connected nodes at the vertices of face-sharing Archimedean polyhedra include: sodalite (truncated octahedron [TO]), Type A zeolite (TO and truncated cuboctahedron [TCO]), faujasite (TO and hexagonal prism [H′]), Mobil ZK5 zeolite (TCO and H′), and Esso Rho zeolite (TCO and octagonal prism). Nets with complex connectivity were developed by systematic removal one-by-one of planes of symmetry. Net 214 is related to fluorite by Ca → cube and F → tetrahedron.

Introduction

The 4-connected frameworks of gmelinite (#82) and chabazite (#83) were obtained in paper II of this series from the 4.6.12 net (Smith, 1978), and the framework of cancrinite (#95) in paper III (Smith, 1979). The present paper provides a systematic enumeration of the infinite set of *ABC*-6 nets obtained by linking parallel 6-rings by tilted 4-rings, and the set of nets related to face-sharing Archimedean polyhedra. Reference is made to the stereo-views in "Atlas of Zeolite Structure Types" by Meier and Olson (1978).

Enumeration of ABC nets

The 4.6.12 2D net provides two distinct positions *A* and *B* for the projection of the 6-rings of a 3D framework (Smith, 1978, Fig. 7), and each 4-ring of the 2D net can be transformed into a tilted 4-ring of the framework. For convenience, consider a framework in which the nodes lie at the corners of regular hexagons and squares, even though this regularity is not necessary from the topological viewpoint. Each regular hexagon of the framework projects vertically onto a regular hexagon of the horizontal 2D net, but each tilted 4-ring projects as a rectangle whose edge ratio is the cosine of the angle of tilt from the horizontal. Hence a regular 2D net must be compressed to represent the projection of a 3D framework composed of regular polygons.

Only one framework is obtained from single hexagons of type *A* and *B* alternating with tilted 4-rings, and this is found in *cancrinite*. Two adjacent planar 6-rings are linked by three pairs of zig-zag 4-rings to form the cancrinite cage (Meier and Olson, p. 23), which is completed by three boat-shaped 6-rings. Each planar 6-ring is shared by two parallel cages and successive face-sharing yields a cancrinite column. Adjacent columns are dove-tailed across the 4-rings to give a 3D framework containing cylindrical channels spanned by 12-rings. The cancrinite framework can be denoted *AB* where *A* and *B* represent the two positions for the 6-rings, and it is understood that a tilted 4-ring lies between symbols.

The *gmelinite* net (Table 1, #82) is obtained from the cancrinite net by replacing each hexagon with an Archimedean hexagonal prism (Meier and Olson, 1978, p. 43). It can be denoted *AABB*. Hexagons of the same type are separated by six vertical 4-rings, whereas hexagons of different types are separated by three tilted 4-rings. Replacement of a hexagon by an Archimedean hexagonal prism corresponds to the sigma-transformation of Shoemaker *et al.* (1973). The gmelinite cage consists of two hexagons suspended between three triplets of edge-shaped squares, thereby generating three boat-shaped 8-rings.

The centers of the hexagons in the cancrinite net and of the hexagonal prisms in the gmelinite net are connected topologically in the same way as the centers of spheres in hexagonal closest-packing. By analogy the *ABC* connectivity of spheres in cubic closest-packing leads to the *ABC* arrangement of parallel spheres in *sodalite* (Table 1, #108) and the *AABBCC* arrangement in *chabazite* (Table 1, #83). Just as for cubic closest-packing of spheres, the unit cell of sodalite is isometric (Meier and Olson, 1978, p. 81), and each hexagon is perpendicular to a triad axis; furthermore the 4-connected nodes lie at the vertices of a closest-packed array of parallel truncated octahedra. The sodalite net is therefore a member of the Archimedean 4-connected nets (next section). In the chabazite net (Meier and Olson, 1978, p. 25), each corner of the rhombohedral unit cell lies at the center of a hexagonal prism, and cages are connected by non-planar 8-rings. Each cage contains two opposing hexagons suspended between six pairs of double 4-rings by the edges of six 4-rings. The cages are connected through octagonal windows to form a 3D channel system.

These four nets are merely the simplest members of an infinite series which is now enumerated. The positional symbols *A*, *B* and *C* are less convenient than operators *s*, *a* and *c* because the starting choice of *A*, *B* and *C* is purely arbitrary. Let *s* (for same) map each hexagon of one horizontal layer onto a hexagon of the next layer to produce a hexagonal prism. The symbol *s* stands for either *AA* or *BB* or *CC*. Change of horizontal position can involve either a clockwise operation (*c*) or an anticlockwise one (*a*), and a tilted 4-ring is involved in both operations. The alphabetical order $A \rightarrow B$, $B \rightarrow C$, $C \rightarrow A$ is clockwise and $A \rightarrow C$, $C \rightarrow B$, $B \rightarrow A$ is anticlockwise. Because of the mirror symmetry of a 4.6.12 net, there is no topological difference between a particular sequence and its $a \rightarrow c$ equivalent; thus *aacac* is topologically equivalent to *ccaca*. Furthermore, the direction and starting point of a sequence are meaningless: thus *aacac* ≡ *cacaa* ≡ *acaca*. For ease of enumeration, it is desirable to arrange a sequence in a standard order. Sequences are grouped first in order of repeat length and number of *s* operators, and then arranged so that *s* precedes *c*, and *c* precedes *a*, whenever a choice is allowed.

The only restriction on sequences is that adjacent *s* operators are not allowed. To make an enumeration for a particular repeat number *p*, first determine the maximum number of *s* operators; this is $p/2$ when *p* is even, and $(p - 1)/2$ when *p* is odd. Insert *c* operators between the *s* operators, and then systematically replace *c* operators by *a* operators one by one from the right of the sequence and move them successively to the left. Check that each new sequence is not merely a cyclic or interchanged version of an earlier sequence. Then remove the *s* operators successively, and repeat the replacement of *c* by *a* operators for each stage.

In order to close a sequence so that the unit cell has the geometry of a 120° hexagonal prism, $(n_c - n_a)$ must equal 3m, where m is an integer, and n_c and n_a are the numbers of clockwise and anticlockwise changes. A complication arises for sequences whose prismatic cell is triply-primitive, and which can be represented by a rhombohedral cell with one-third the volume of the prismatic cell. Thus the levyne sequence *sccsccscc* corresponds to a 9-repeat hexagonal prism (Meier and Olson, 1978, p.51), while the *scc* triplet corresponds to the inclined edge of a rhombohedral unit cell. The topological "complexity" of the levyne sequence is expressed just by the triplet *scc*, and levyne has a less complex sequence than liottite (Meier and Olson, 1978, p.53) whose *ccacaa* sequence requires a 6-repeat prismatic cell. A rhombohedral cell is obtained only for sequences whose prismatic repeat is 3q, where q is an integer, and for which the positions repeat cyclically at r, (r + q) and (r + 2q). Thus levyne has the rhombohedral sequence *AAB(CCA)(BBC)*. For sodalite with *ccc* = *ABC*, the 3-layer prismatic cell reduces to the 1-layer rhombohedral cell represented formally by *c* = *A*; because of special geometrical relations, the rhombohedral cell is actually isometric. The *cacaca* sequence does not give a rhombohedral cell because the *ABA BAB* sequence corresponds to three prismatic cells of *AB*.

Table 1 lists prismatic repeats up to 8, and rhombohedral repeats up to 5. Rhombohedral sequences are denoted by a star, and the sequence of operators is expressed as $(\dots)^3$. The comments provide hints on the process of enumeration. A computer program was written, and a copy of the sequences up to a prismatic repeat of 11 can be obtained from J. M. Bennett (9 repeat, 96 sequences; 10, 230; 11, 529. The proposed 10-layer sequence of *ABCABCBACB* of franzinite (see below) has been designated #201, but numbers have not been given to sequences not listed in Table 1. The enumeration in Table 1 corresponds to "coloring" a trigonal rod group so that each triangle has two unoccupied vertices and one occupied vertex.

The highest space group and the circuit symbol are listed in Table 2 for each ideal framework. The circuit symbols can be obtained from the operators by the following procedure: (i) replace *a* and *c* by a dot, (ii) read off the circuit symbol from the following table, where the dagger denotes the position of a node for which the symbol is derived:

s†.s	$4^3 6^2 8$	e
s†..	$4^3 6^3$	d
s.†.s	$4^2 6^2 8^2$	h
s.†..	$4^2 6^3 8$	g
..†..	$4^2 6^4$	f

For brevity, the numerical circuit symbols are denoted by d–h in Table 2. Readers can deduce the types of cages in a particular net by using the following key:

s	hexagonal prism
ca	cancrinite
ccc	sodalite
csa	offretite (or gmelinite)
ccaa	losod
ccsc	levyne
cscsc	chabazite

The space group can be determined analytically. Rhombohedral sequences have a vertical mirror plane and only $R3m$ and $R\bar{3}m$ need consideration. A center of symmetry indicates $R\bar{3}m$. Thus sequence *AABCABBCABCCABC* (#196) has a center of symmetry between the first and second *A*, and at the fourth *A*; each center maps *A* onto *A*, and *B* onto *C*. A vertical mirror plane in the first position is present in all prismatic sequences, and a rotation hexad is not allowed. Space group $P6_3/mmc$ is present only for sequences with an even-numbered repeat (p), and then only when $A(\mathrm{v}) \rightarrow A(\mathrm{v} + p/2)$ and $B(\mathrm{w}) \rightarrow C(\mathrm{w} + p/2)$, or a cyclic equivalent, where v and w are any positions in a sequence of layers. Thus sequence *ABCB* (#110) with $p = 4$ has $A(1) \rightarrow C(3)$ and $B(2) \rightarrow B(4)$. The only remaining space groups with a vertical mirror plane in the first position are $P\bar{3}m1$, $P3m1$ and $P\bar{6}m2$. Because $\bar{6} \equiv 3/m$, the presence of a horizontal mirror plane provides an easy criterion for assignment of $P\bar{6}m2$; thus in *AAB* (#106) mirror planes pass mid-way between the two *A*'s and directly through *B*. The remaining sequences go into $P\bar{3}m1$ if a center of symmetry is present, and into $P3m1$ if not; thus *AABAC* (#114) has a center between the first two *A*'s and at the third *A*, and *B* is mapped onto *C* by them.

All observed members of the *ABC*-6 family (Table 3) have relatively simple connectivity with respect to unobserved members. Nine unobserved members with fairly simple stacking and high symmetry are listed in the abstract.

There are many structural complexities in the observed members. Chabazite gives X-ray diffractions consistent with *AABBCC* stacking (Dent and Smith, 1958), and the reduction of symmetry below the ideal space group $R\bar{3}m$ results from cation positions and not from the topology. Stacking faults (*e.g., AABBAA*) would lead to twinning on hexagonal (0001), and are presumably responsible for the interpenetrant rhombohedral habit. Gmelinite with ideal *AABB* stacking (Dent and Smith, 1958) shows frequent stacking faults (Fischer, 1966) which are presumed to be at least mainly of *AABBCC* type, but which require further study by electron microscopy. Offretite (*AAB*) and erionite (*AABAAC*) were not originally distinguished as separate minerals, but combined X-ray and electron-optical studies have revealed the ideal stacking sequences and faults (Bennett and Gard, 1967; Kawahara and Curien, 1969; Gard and Tait, 1971, 1972; Kokotailo *et al.*, 1972) and microprobe analyses (Sheppard *et al.*, 1974; Rinaldi, 1976) have demonstrated a chemical relation to the stacking sequence. Levyne (*AABCCABBC*) occurs intergrown with offretite (Sheppard *et al.*, 1974), and channel systems are compared for levyne and related zeolites in Barrer and Kerr (1959).

The term cancrinite-like has been applied to various feldspathoid minerals that do not have the *ABC* stacking of sodalite. Ideal cancrinite has *AB* stacking (Jarchow, 1965), and framework ordering reduces the symmetry to $P6_3$. Complications arise from ordering of the channel constituents in a framework with *AB* stacking, and superstructures with *c* increased by 5, 8, 11, 16 and 27 have been observed (Brown and Cesbron, 1973; Foit *et al.*, 1973). The superstructure diffractions lose intensity upon heating in response to increasing disorder of channel constituents. Microsommite has a superstructure with *a* increased by $\sqrt{3}$. Complex stacking variations were imaged electron-optically by Rinaldi and Wenk (1979), and partly published studies have characterized liottite (*ABABAC*) and afghanite (Merlino and Mellini, 1976). Furthermore Rinaldi and Wenk state that franzinite

Table 1. Enumeration of simpler nets of the *ABC* family

Operators	Positions	No.	Comment
2 layers (1 possibility)			
ca	AB	95	s not possible
3 layers (2 possibilities)			
sca	AAB	106	only choice for one s
$*(c)^3$	ABC	108	≡ aaa; *actually isometric
4 layers (3 possibilities)			
scsa	AABB	82	only choice for two s
sccc	AABC	109	≡ saaa
ccaa	ABCB	110	
[caca]; [scsc]			reduces to two ca and sc
5 layers (5 possibilities)			
scscc	AABBC	111	≡ sasaa; only choice for 2s
sccaa	AABCB	112	adjacent c
scaca	AABAB	113	one apart
scaac	AABAC	114	two apart; ≡ sacca
cccca	ABCAB	115	≡ aaaac
6 layers (10 possibilities)			
$*(sc)^3$	AABBCC	83	≡ rhombohedral sc
scscaa	AABBCB	116	s one apart; second c at front
scsaca	AABBAB	117	do. ; second c in middle
sccsaa	AABCCB	118	s two apart; two c at front
[scasca]			reduces to two sca
scasac	AABAAC	119	≡ sacsca
scccca	AABCAB	120	one s; four c at front
scccac	AABCAC	121	do. ; a moves forward
sccacc	AABCBC	122	do.
cccaaa	ABCACB	123	no s; three c at front
ccacaa	ABCBCB	124	≡ ccaaca
[cacaca]			reduces to three ca
7 layers (20 possibilities)			
scscsaa	AABBCCB	125	three s; two a at end
scsasca	AABBAAB	126	do. ; ca at end
scsasac	AABBAAC	127	do. ; ac at end
scsccca	AABBCAB	128	two s one apart; a at end
scsccac	AABBCAC	129	≡ scsccac
sascccc	AACCABC	130	
sccscca	AABCCAB	131	two s two apart; a at end
sccscac	AABCCAC	132	do. ; a in middle
scasccc	AABAABC	133	≡ sacsccc
scccccc	AABCABC	134	one s; ≡ saaaaaa
scccaaa	AABCACB	135	do. ; ccc at front
sccacaa	AABCBCB	136	do. ; third c moves
sccaaca	AABCBAB	137	do. ; do.
sccaaac	AABCBAC	138	do. ; do.
scacaca	AABABAB	139	third c moves
scacaac	AABABAC	139a	scaccaa ≡ sccaaca
scaacca	AABACAB	140	second c moves
cccccaa	ABCABCB	141	no s; five c at front
ccccaca	ABCABAB	142	fifth c can only move once
cccacca	ABCACAB	143	fourth c can only move once
8 layers (45 possibilities)			
scscsasa	AABBCCBB	144	four s must alternate
[scsascsa]			reduces to two scsa
scscscca	AABBCCAB	145	1,1,3 between s; a at end
scscscac	AABBCCAC	146	do. ; a moves
scsasccc	AABBAABC	147	do. ; do.
scsccsca	AABBCAAB	148	1,2,2 between S; a at end
scsccsac	AABBCAAC	149	do. ; move a
sasccscc	AACCABBC	150	do. ; do.
scsccccc	AABBCABC	151	1,5 between s; six c
scsccaaa	AABBCACB	152	do. ; three c at front
scscacaa	AABBCBCB	153	do. ; last c moves
scscaaca	AABBCBAB	154	do. ; do.
scscaaac	AABBCBAC	155	do. ; do.
scsaccaa	AABBABCB	156	do. ; next c moves
scsacaca	AABBABAB	157	do. ; last c moves
sccscccc	AABCCABC	158	2,4 between s; six c
sccscaaa	AABCCACB	159	do. ; three c at front
sccsacaa	AABCCBCB	160	do. ; last c moves
scasccaa	AABAABCB	161	do. ; middle c moves
scascaca	AABAABAB	162	do. ; last c moves
scasacca	AABAACAB	163	do. ; middle c moves
scasacac	AABAACAC	164	do. ; last c moves
scasaacc	AABAACBC	165	do. ; middle c moves
[scccsccc]			reduces to two sccc
scccsaaa	AABCAACB	166	3,3 between s; three c at front

(Merlino and Orlandi, 1977) was found to have *AB CABCBACB* stacking by Merlino and Mellini.

To a first approximation, all silicates belonging to the *ABC*-6 family have X-ray diffraction patterns which can be indexed on a hexagonal prismatic cell with $a \sim 13.0\pm0.3$Å and $c \sim p \times (2.6\pm0.1)$Å. Rhombohedral varieties have systematic absences for $(h - k) \neq 3n$. Because the angle of tilt of the 4-rings depends on chemical interactions between framework and non-framework species, there is not a unique relation between cell dimensions and the ratio of s to $(c + a)$ operators. However, existing data on cell dimen-

Table 1. (continued)

Operators	Positions	No.	Comment
sccascaa	AABCBBCB	167	3,3 between s; last c moves
sccasaca	AABCBBAB	168	do. ; do.
sccasaac	AABCBBAC	169	do. do.
[scacscaa]			≡ sccasaca
scacsaca	AABABBAB	170	do. ; middle c moves
scccccaa	AABCABCB	171	one s; five c at front
scccaca	AABCABAB	172	do. ; fifth c moves
scccaac	AABCABAC	173	do. ; do.
scccacca	AABCACAB	174	do. ; fourth c moves
scccacac	AABCACAC	175	do. ; fifth c moves
scccaacc	AABCACBC	176	do. ; fourth c moves
sccaccca	AABCBCAB	177	do. ; third c moves
sccaccac	AABCBCAC	178	do. ; fifth c moves
sccacacc	AABCBCBC	179	do. ; fourth c moves
scaccca	AABABCAB	180	do. ; second c moves
scacccac	AABABCAC	181	do. ; fifth c moves
sacccca	AACABCAB	182	do. ; first c moves
ccccaaaa	ABCABACB	183	no s ; four c at front
cccacaaa	ABCACACB	184	do. ; fourth c moves
cccaacaa	ABCACBCB	185	do. ; do.
[ccaccaaa]			≡ cccaacaa
ccacacaa	ABCBCBCB	186	do. ; fourth c moves
ccacaaca	ABCBCBAB	187	do. ; do.
[cacacaca]			≡ four ca
cccccca	ABCABCAB	188	do. ; seven c at front
9 layers prismatic (3 layers rhombohedral)			
$*(scc)^3$	AABCCABBC	189	one s; sca is prismatic
$*(cca)^3$	ABCBCACAB	190	no s ; only possibility
12 layers prismatic (4 layers rhombohedral)			
$*(scca)^3$	AABCBBCACCAB	191	$[sc]^6$ is chabazite
$*(scac)^3$	AABABBCBCCAC	192	$[scsa]^3$ is prismatic
$*(ccca)^3$	ABCACABCBCAB	193	
15 layers prismatic (5 layers rhombohedral)			
$*(scsca)^3$	(AABBC)B..C..	194	$[scscc]^3$ is prismatic
$*(sascc)^3$	(AACCA)B..C..	195	
$*(scccc)^3$	(AABCA)B..C..	196	note A→B→C
$*(sccca)^3$	(AABCA)C..B..	197	note A→C→B
$*(sccac)^3$	(AABCB)C..B..	198	$[sccaa]^3$ is prismatic
$*(cccaa)^3$	(ABCAC)B..C..	199	$[scaca]^3$ is prismatic
$*(ccaca)^3$	(ABCBC)B..C..	200	

sions of *ABC*-6 structures suggest that the function pa/c increases from ~4.9 when s is zero to ~5.5 when s is highest, with ~5.2–5.3 for intermediate values of $s/(c + a)$. This observation by J. A. Gard in Shoemaker *et al.* (1973) should be useful in a preliminary examination of cell dimensions of a new phase. The pa/c value of 4.8 for franzinite is consistent with absence of an s operator in the proposed *ABCABC BACB* sequence. Caution is needed in comparing the space group and diffraction intensities of an unknown material with the space group and calculated diffraction intensities for a theoretical sequence with idealized geometry.

Enumeration of 4-connected Archimedean nets

The sodalite net (#108) has tetrahedral nodes at the vertices of a space-filling array of closest-packed truncated octahedra; indeed this Archimedean polyhedron is one of the five parallelohedra (or Fedorov solids) that can fill space completely just by translation. The present enumeration of 4-connected nets whose nodes lie at the corners of Archimedean polyhedra is based on Moore and Smith (1964) with a correction in Moore and Smith (1967). Space filling by Archimedean polyhedra was described by Andreini (1907).

The Archimedean polyhedra contain regular faces, not all of the same kind, arranged in the same order around each vertex. Six polyhedra, and the infinite series of antiprisms, have four edges meeting at each vertex, and cannot be used to generate 4-connected 3D nets because additional edges would appear upon joining polyhedra together. Polyhedra with pentagonal faces cannot share faces to generate a 4-connected net with lattice symmetry: however, the pentagonal dodecahedron can share faces with 14-, 15-, and 16-dedra ($5^{12}6^{2-4}$) to form nets in gas hydrates (Wells, 1975, p. 544); furthermore the sodalite net is the basis of type (a) gas hydrates. The truncated tetrahedron and truncated cube were discarded by Moore and Smith because of their 3-rings; however they combine with a truncated cuboctahedron to give net 207a (Table 4). Of principal interest are the truncated octahedron (TO), truncated cuboctahedron (TCO), and the prisms, of which the hexagonal prism (H′) and octagonal prism (O′) are the only ones needed. The cube (C), which is a Platonic solid, is also useful for description. Square, hexagonal and octagonal contacts are denoted S, H and O. The possible nets are enumerated from systematic consideration of all ways of placing faces in contact, combined with all combinations of opposing faces from the attached polyhedra. A simple description lists the types of adjacent polyhedra, the type of contact, and the types of faces opposing across the contact. Thus sodalite is (TO, 6)–S–(TO, 6). For convenience, C, H′ and O′ will also be listed as contacts.

Table 2. Simpler nets of the *ABC* family

No.	Z_t	Circuit symbol	Z_c	Highest space group	Hexagonal c(Å)	No.	Z_t	Circuit symbol	Z_c	Highest space group	Hexagonal c(Å)	No.	Z_t	Circuit symbol	Z_c	Highest space group	Hexagonal c(Å)
95	12	f_2	12	$P6_3/mmc$	5	137	42	dgfffgd	42	$P3m1$	17.5	169	48	dggddggd	48	$P6_3/mmc$	20
106	18	ddh	18	$P\bar{6}m2$	7.5	138	42	do.	42	$P3m1$	17.5	170	48	dggddggd	48	$P6_3/mmc$	20
108	6	f_3	12	$I\bar{4}3m$	(cubic) 9	139	42	do.	42	$P\bar{6}m2$	17.5	171	48	gffffffg	48	$P3m1$	20
82	24	e_4	24	$P6_3/mmc$	10	139a	42	do.	42	$P3m1$	17.5	172	48	do.	48	$P3m1$	20
109	24	dg	24	$P\bar{3}m1$	10	140	42	do.	42	$P\bar{6}m2$	17.5	173	48	do.	48	$P3m1$	20
110	24	f_4	24	$P6_3/mmc$	10	141	42	f_7	42	$P\bar{3}m1$	17.5	174	48	do.	48	$P3m1$	20
111	30	eedhd	30	$P3m1$	12.5	142	42	do.	42	$P\bar{3}m1$	17.5	175	48	do.	48	$P3m1$	20
112	30	dgfgd	30	$P\bar{6}m2$	12.5	143	42	do.	42	$P\bar{3}m1$	17.5	176	48	do.	48	$P3m1$	20
113	30	do.	30	$P\bar{6}m2$	12.5	144	48	e_8	48	$P6_3/mmc$	20	177	48	do.	48	$P3m1$	20
114	30	do.	30	$P\bar{3}m1$	12.5	145	48	eeeedggd	48	$P3m1$	20	178	48	do.	48	$P3m1$	20
115	30	f_5	30	$P3m1$	12.5	146	48	do.	48	$P\bar{3}m1$	20	179	48	do.	48	$P\bar{3}m1$	20
83	12	e_6(e_2 rh)	36	$R\bar{3}m$	15	147	48	do.	48	$P3m1$	20	180	48	do.	48	$P3m1$	20
116	36	eedggd	36	$P3m1$	15	148	48	eedhddhd	48	$P3m1$	20	181	48	do.	48	$P\bar{3}m1$	20
117	36	do.	36	$P3m1$	15	149	48	do.	48	$P3m1$	20	182	48	do.	48	$P\bar{3}m1$	20
118	36	dhddhd	36	$P6_3/mmc$	15	150	48	do.	48	$P\bar{3}m1$	20	183	48	f_8	48	$P6_3/mmc$	20
119	36	do.	36	$P6_3/mmc$	15	151	48	eedgffgd	48	$P\bar{3}m1$	20	184	48	do.	48	$P\bar{6}m2$	20
120	36	dgffgd	36	$P3m1$	15	152	48	do.	48	$P3m1$	20	185	48	do.	48	$P\bar{3}m1$	20
121	36	do.	36	$P3m1$	15	153	48	do.	48	$P3m1$	20	186	48	do.	48	$P\bar{6}m2$	20
122	36	do.	36	$P\bar{3}m1$	15	154	48	do.	48	$P3m1$	20	187	48	do.	48	$P6_3/mmc$	20
123	36	f_6	36	$P6_3/mmc$	15	155	48	do.	48	$P\bar{3}m1$	20	188	48	do.	48	$P3m1$	20
124	36	do.	36	$P\bar{6}m2$	15	156	48	do.	48	$P3m1$	20	189	18	dhd (rh)	54	$R\bar{3}m$	22.5
125	42	eeeedhd	42	$P\bar{3}m1$	17.5	157	48	do.	48	$P\bar{3}m1$	20	190	18	f_3	54	$R\bar{3}m$	22.5
126	42	do.	42	$P\bar{6}m2$	17.5	158	48	dhddgfgd	48	$P\bar{3}m1$	20	191	24	dggd	72	$R3m$	30
127	42	do.	42	$P\bar{6}m2$	17.5	159	48	do.	48	$P3m1$	20	192	24	do.	72	$R\bar{3}m$	30
128	42	eedgfgd	42	$P3m1$	17.5	160	48	do.	48	$P3m1$	20	193	24	f_4	72	$R\bar{3}m$	30
129	42	do.	42	$P3m1$	17.5	161	48	do.	48	$P\bar{6}m2$	20	194	30	eedhd	90	$R3m$	37.5
130	42	do.	42	$P3m1$	17.5	162	48	do.	48	$P\bar{6}m2$	20	195	30	do.	90	$R3m$	37.5
131	42	dhddggd	42	$P3m1$	17.5	163	48	do.	48	$P3m1$	20	196	30	dgfgd	90	$R\bar{3}m$	37.5
132	42	do.	42	$P3m1$	17.5	164	48	do.	48	$P\bar{6}m2$	20	197	30	do.	90	$R3m$	37.5
133	42	do.	42	$P3m1$	17.5	165	48	do.	48	$P\bar{6}m2$	20	198	30	do.	90	$R3m$	37.5
134	42	dgfffgd	42	$P\bar{3}m1$	17.5	166	48	dggddggd	48	$P6_3/mmc$	20	199	30	f_5	90	$R3m$	37.5
135	42	do.	42	$P\bar{6}m2$	17.5	167	48	do.	48	$P\bar{6}m2$	20	200	30	do.	90	$R3m$	37.5
136	42	do.	42	$P\bar{6}m2$	17.5	168	48	do.	48	$P3m1$	20	201	60	f_{10}	60	$P3m1$	25

Z_t number of tetrahedra in a symmetric unit. Z_c number of tetrahedra in unit cell.

Face-sharing of prisms does not yield 4-connected 3D nets. The truncated octahedron can share square faces in only one way to give the sodalite net. The hexagonal faces can be shared in two ways because of alternation of square and hexagonal faces around each hexagonal face. Sodalite can also be described as (TO, 4)–H–(TO, 6). Certain combinations of linkage do not yield frameworks because of unsuitable angles: thus (TO, 4)–H–(TO, 4) does not yield a net by itself. However, net 183 of the *ABC*-6 family can be generated by deliberate use of both (4)–H–(4) and (4)–H–(6); adjacent faces perpendicular to the *c*-axis are (4)–(4) and ones inclined to *c* are (4)–(6). The Type A zeolite (Meier and Olson, 1978, p. 57) results from (TO, 6)–C–(TO, 6). A TO lies at each corner of a primitive unit cell, a regular hexahedron at the mid-point of each edge, and a TCO at the body-center. Alternative descriptions for zeolite A are (TCO, 4)–O–(TCO, 4), (TCO, 6)–C–(TCO, 6) and (TO, 4)–H–(TCO-4).

The faujasite net (TO, 4)–H′–(TO, 6) can be obtained by replacing each C atom of diamond with a TO (Meier and Olson, 1978, p. 37). Replacement of each shared hexagonal face by a hexagonal prism in net 183 yields net 204 whose TO match the C atoms in lonsdaleite. An infinite polytypic series, analogous to the diamond–lonsdaleite (or blende–wurtzite) series, can be derived from the faujasite net. Natural faujasite and synthetic relatives commonly crystallize as interpenetrating octahedra twinned on (111), and the twin interface presumably results from a planar array of hexagonal prisms with (4)–(4) linkage. The faujasite net contains a wide 3D channel system whose intersections generate a 26-hedron with four hexagons, eighteen squares and four non-planar dodecagons as faces, and net 204 contains cages composed of six hexagons, 21 squares, two regular dodecagons and three boat-shaped ones.

The net of the Mobil ZK5 zeolite (Meier and Olson, 1978, p. 47) is obtained by linking hexagonal

Table 3. Observed members of the *ABC* family

Type	Name	Reference	S. G.	a(Å)	c(Å)
82	gmelinite	see paper II	$P6_3/mmc$	13.7	10.0
83	chabazite	do.	$R\bar{3}m$?	13.2	15.1
95	cancrinite	see paper III	$P6_3$	12.7	5.1
106	offretite	do.	$P\bar{6}m2$	13.3	7.6
108	sodalite	see Table 4			
110	losod	Sieber & Meier (1974)	$P\bar{6}2c$	12.9	10.5
118	TMA-E(AB)	Groner & Meier (1979)	$P6_3/mmc$	13.3	15.2
119	erionite	Staples and Gard (1959)	$P6_3/mmc$	13.3	15.1
124	liottite	Merlino & Orlandi (1977)	$P\bar{6}m2$	12.8	16.1
187	afghanite	Bariand et al. (1968)	a	12.8	21.3
189	levyne	Merlino et al. (1975)	$R\bar{3}m$	13.34	23.01
201	franzinite	Merlino and Orlandi (1977)	b	12.88	26.58

a $P6_3/mmc$ or $P6_3mc$ or $P\bar{6}2c$. b $P\bar{3}m1$ or $P3m1$ or $P321$.

faces of adjacent TCO by (4)–H′–(8). In addition to the TCO cage, there is a cage comprised of two octagons, four sets of three squares, and four boat-shaped octagons, which can be obtained from the gmelinite cage by increasing the symmetry from 3-fold to 4-fold. The net of the Esso Rho zeolite is obtained by joining TCO either (4)–O′–(4) or (4)–H–(8). The entire volume is filled by TCO and OP (Meier and Olson, 1978, p. 79).

Truncated octahedra and truncated cuboctahedra can be linked in only two ways to form 4-connected nets. The linkage (4)–H–(4) gives the net of the A zeolite, and the linkage (4)–H′–(4) gives net 207 in which each F atom of the fluorite structure is replaced by a TO and each Ca atom by a TCO. Each face-centered cubic cell contains 384 tetrahedral nodes, and the Archimedean polyhedra surround 4 large cages. Each is defined by 24 squares, 8 hexagons, 6 regular octagons and 12 elongated octagons, and this 50-hedron with $m3m$ point symmetry is considerably larger than the 26-hedron of the faujasite net. Elongated O′ also occur. Net 207 is not represented by either a natural or synthetic material.

The net of paulingite (Meier and Olson, 1978, p. 75) contains TCO and O′, but it is not listed here as an Archimedean net because a non-Archimedean cage links the Archimedean polyhedra. This cage is the 18-hedron found in ZK5, and the net of paulingite can be symbolized as (TCO, 4)–O′–(18h, 4)–O′–(18h, 4)–O′–.

Enumeration of 4-connected near-Archimedean nets

Shoemaker *et al.* (1973) developed the A and rho nets from the sodalite net by addition of a mirror plane in successive σ-transformations. The approach by Moore and Smith automatically produced nets with a symmetrical arrangement of σ-transformations, and the less-symmetrical arrangements (Table 5) are now determined.

A TCO with attached O′ (Fig. 1) contains six mirror operations when linked into an infinite array as in the rho net (#206). It can be transformed into a TO of the sodalite net (#108) by removal of the six mirror operations. Shoemaker *et al.* enumerated all the simple nets obtained by removal of one to five mirror operations from net 206. Each σ operation in the waist of an O′ is labeled with a subscript 1, 2 or 3 to denote the arbitrary choice of *a, b* and *c* reference axes, and corresponding σ operations passing through the centroid of a TCO in Figure 1 are labeled 4, 5 and 6. The distinction between subscripts 1 and 4 is merely formal in the rho net because each σ operator passes through the waist of an O′ and then passes through the centroid of an adjacent TCO; however, it becomes meaningful if a distinction is made between positions 2 and 5, or 3 and 6. Shoemaker *et al.* assigned arbitrary Greek letters α-π, and the sequence 208–217 follows that order. However, it is convenient to follow a different sequence in which σ-operations are added successivly to the sodalite net (Table 6).

Nets 208 and 209 contain a TCO and nets 210 and 211 contain a TO. All nets contain either one or two non-Archimedean polyhedra with 18 to 22 faces (Table 5). Each of these polyhedra contains eight hexagons which survive from the TO of the sodalite net, and a variety of S, H and O faces which depends on the number of σ-operations applied to the original

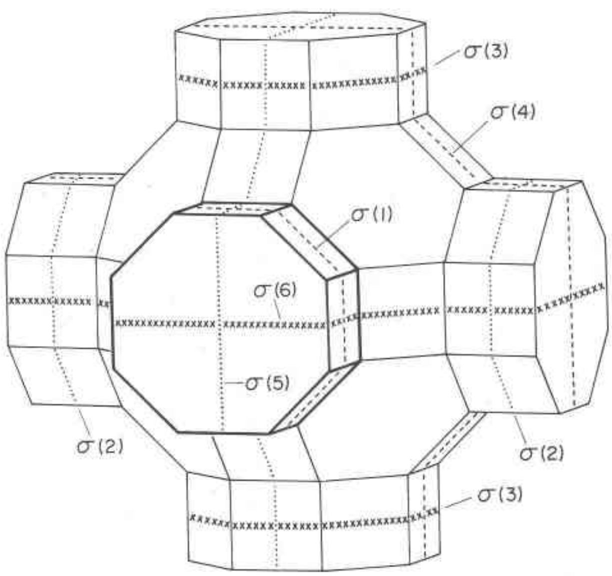

Fig. 1. The six types of σ-transformations for a truncated cuboctahedron with attached octagonal prisms.

Table 4. Simple 4-connected nets based on Archimedean polyhedra

No.	Z_t	Circuit symbol	Z_c	Highest space group	Cell edge (Å)	Connectivity	Polyhedra
108	6	4^26^4	12	Im3m	9	(TO, 6)-S-(TO, 6)	TO
183	48	4^26^4	48	$P6_3/mmc$	a 13, c 20	(TO, 4)-H-(TO, 4 and 6)	TO
202	24	4^36^28	24	Pm3m	12	(TO, 6)-C-(TO, 6)	TO, TCO, C
203*	48	4^36^3	192	Fd3m	25	(TO, 4)-H'-(TO, 6)	TO, H', 26h
204*	96	4^36^3	96	$P6_3/mmc$	a 17, c 27	(TO, 4)-H'-(TO, 4 and 6)	TO, H', 32h
205	48	4^36^28	96	Im3m	19	(TCO, 4)-H'-(TCO, 8)	TCO, H', 18h
206	24	4^36^3	48	Im3m	15	(TCO, 4)-H-(TCO, 8)	TCO, O'
207	96	$(4^36^3)_1(4^36^28)_1$	384	Fm3m	31	(TO, 4)-H'-(TCO, 4)	TCO, TO, H', DOP
207a	24	$3,4,6^28^2$	96	Fm3m	19	(TCO, 4)-O-(TC, 8); (TCO, 8)-H-(TT, 3)	TCO, TC, TT

*Two simplest members of infinite polytypic series analogous to diamond and lonsdaleite. TO truncated octahedron; TT truncated tetrahedron; TCO truncated cuboctahedron; H' hexagonal prism; O' octagonal prism; DOP distorted octagonal prism; C cube; h hedron.

Type	Name	Reference	Space Group	Cell Edge
108	sodalite group	Barth (1937); Taylor (1967)	$P\bar{4}3n$	8.9
108	helvine	Holloway et al. (1972)	$P\bar{4}3n$	8.3
108	bicchulite	Sahl (1980)	$I\bar{4}3m$	8.8
108	tugtupite	Danø (1966)	$I\bar{4}$	8.6
202	type A	Reed & Breck (1956); Gramlich & Meier (1971)	$Fm\bar{3}c$	24.6
203	faujasite	Bergerhoff et al. (1958)	Fd3m	24.7
205	Mobil ZK5	Meier & Kokotailo (1965)	Im3m	18.7
206	Esso rho	Robson et al. (1973)	$I\bar{4}3m$?	15.1

square faces of the TO. All nets also enclose one or more C, H′ and O′ polyhedra.

Net 214 (Fig. 2) is remarkable because of its face-centered cubic symmetry and small value of Z_t. During algebraic enumeration, it was expected that the 14 positions of the σ operators would lead to tetragonal symmetry, but examination of a model revealed that net 214 can be constructed by replacing each F atom of the fluorite structure by a cube of linked tetrahedra. Each Ca atom is replaced by a tetrahedral node, and each of the four branches is linked to a tetrahedral node at the vertex of a neighboring cube. The cage is a truncated rhombic dodecahedron, and the net can be developed from a $46^2,6^4$ 2D tessellation. Nets 211 and 216 also have small values of Z_t.

Figure 3 shows how the 3D nets can be described with reference to 2D nets. The sodalite, A and rho nets respectively project onto nets with the following nodes; 46^2 and 6^4; 46^2 and 468; 4^36 and 468. Not all the polygons are regular, and even greater complexity is found for the projected nets 211 and 209.

Pairs of 3D nets can form an infinite polytypic series if they have an identical 2D cross-section. Thus the sodalite and 211 nets differ only by a $\sigma(3)$ transformation and the (001) plane provides a fit to yield polytypes with a tetragonal unit cell *a* 9Å*c* (9p + 12q)Å where p and q are integers.

The only other new nets that can be developed from the Archimedean nets in Table 4 by one or more σ-transformations, *each of infinite planar extent*, belong to an infinite polytypic series obtained from net 204. Conversion of each hexagonal prism lying perpendicular to the *c*-axis to a hexagon produces net 218, and intermixing of nets 204 and 208 produces a polytypic series. Whereas each $4^{21}6^612^5$ cage of net 204 is joined to adjacent cages by two near-circular 12-rings and three boat-shaped 12-rings, each $4^{18}6^610^312^2$ cage of net 218 retains the near-circular 12-rings but has three boat-shaped 10-rings. The

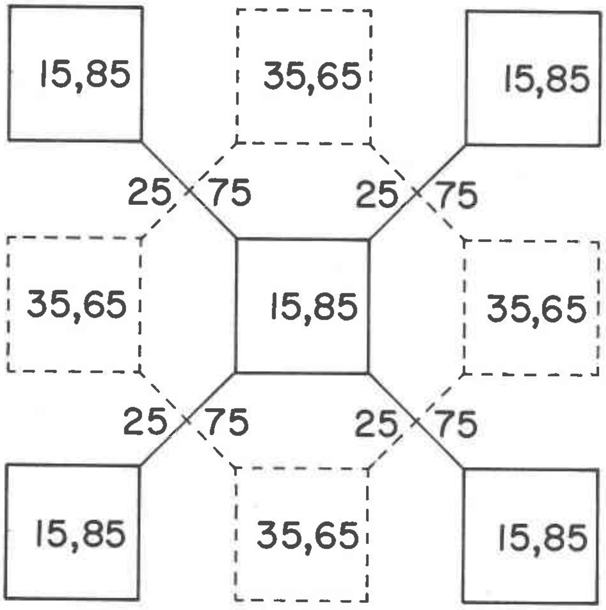

Fig. 2. Projection of net 214. Nodes at height ±15 and ±35 hundredths form cubes whose vertices are linked by branches from nodes at 25 and 75 hundredths.

growth step of 125Å in zeolite ZSM-3 corresponds to a complex polytype (Kokotailo and Ciric, 1971).

Application of a σ^{-1} transformation to individual polyhedra *not lying in a plane* yields further nets. Retention of the perpendicular hexagonal prisms in net 204, and conversion to a hexagon of all the others yields net 219. This net belongs to the ABC-6 series, and would be coded as *sccccsaaaa.* It contains $4^9 6^6 8^3$ and gmelinite-type cages which form a 3D-channel system connected through 8-rings; TO and H′ also occur. Conversion of all the prisms yields net 183 of the ABC-6 series with sequence *ccccaaaa.* A polytypic series can be obtained by inserting *s* only at some of the *ca* boundaries. These σ^{-1}-transformations do not result in angular distortion of TO, but application of a σ^{-1} transformation to all Archimedean nets in Table 4, except as already described, results in distortion. A σ^{-1} transformation can be applied successively to near-planar arrays of H′ in the faujasite net, and four such transformations yield the sodalite net. Because of the distortion, called *pleating* by Shoemaker *et al.,* the three intermediate nets are not listed in Table 5. Similar transformations can be applied to H′ in net 207.

Conclusion

The present investigation systematizes the studies by earlier workers on the ABC-6, Archimedean, and near-Archimedean nets, and demonstrates the cross-relationships. Just as for the nets developed in the earlier papers of this series, natural and synthetic materials tend to assume a framework with simple connectivity. However the occurrence of minerals with 8- and 10-layer repeats in the ABC-6 series provides justification for systematic enumeration of nets with complex connectivity. Just as in organic chemistry, there is an intellectual challenge to find a way to synthesize materials with nets so far known only from mathematical invention. Success might provide materials with valuable physical properties.

Table 5. Complex 4-connected nets based on Archimedean polyhedra

No.	Z_t	Circuit symbol	Z_c	Highest space group	Cell edges Å	Connections	Polyhedra
208	40	$(4^3 6^3)_4 (4^2 6^3 8)_1$	40	P4/mmm	a 14, c 12	σ(1-5)-sodalite	H′,O′,TCO,$4^8 6^{12} 8^2$
209	32	$(4^3 6^3)_2 (4^3 6^2 8)_1 (4^2 6^3 8)_1$	32	P4/mmm	a 12, c 14	σ(1-4)-sodalite	C,H′,O′,TCO,$4^6 6^{12}$
210	20	$(4^3 6^3)_2 (4^3 6^2 8)_2 (46^5)_1$	20	P4/mmm	a 11, c 9	σ(1,2)-sodalite	TO,C,$4^8 6^{12} 8^2$
211	16	$(4^3 6^3)_2 (4^2 6^4)_1 (46^5)_1$	16	P4/mmm	a 9, c 12	σ(3)-sodalite	TO,C,$4^6 6^{12}$
212	22	complex	22	Pmmm	a 12, b 14, c 10	σ(3,5,6)-sodalite	C,H′,$4^8 6^{12} 8^2$,$4^6 6^{12}$
213	28	$(4^3 6^3)_4 (4^2 6^4)_2 (46^5)_1$	28	P4/mmm	a 11, c 11	σ(1,2,6)-sodalite	H′,O′,$4^8 6^{12} 8^2$,$4^6 6^{12}$
214	10	$(4^3 6^3)_4 (6^6)_1$	40	Fm3m	13	σ(1,4)-sodalite	C,$4^6 6^{12}$
215	22	$(4^3 6^3)_4 (4^2 6^4)_5 (46^5)_2$	22	$P4_2$/mmc	a 12, c 9	σ(1,5)-sodalite	H′,$4^6 6^{12}$
216	16	$(4^3 6^3)_1 (4^2 6^3 8)_1$	32	I4/mmm	a 14, c 10	σ(1,2,4,5)-sodalite	H′,$4^8 6^{12} 8^2$
217	34	$(4^3 6^3)_{12} (4^2 6^4)_4 (6^6)_1$	34	$P4_2$/mmc	a 12, c 14	σ(1,2,4,6)-sodalite	H′,O′,$4^8 6^{12} 8^2$
218	84	$(4^3 6^3)_6 (4^2 6^4)_1$	84	$P6_3$/mmc	a 17, c 21	σ^{-1}(H′,0001)-204	H′,$4^{18} 6^6 10^3 12^2$
219	60	$(4^3 6^3)_2 (4^2 6^4)_1 (4^2 6^3 8)_2$	.60	$P6_3$/mmc	a 12, c 25	σ^{-1}(H′, inclined)-204	H′,TO,$4^9 6^6 3^8$,G
183	48	$4^2 6^4$	48	$P6_3$/mmc	a 12, c 20	σ^{-1}(H′)-219	TO,$4^5 6^{11}$

G gmelinite-type cage

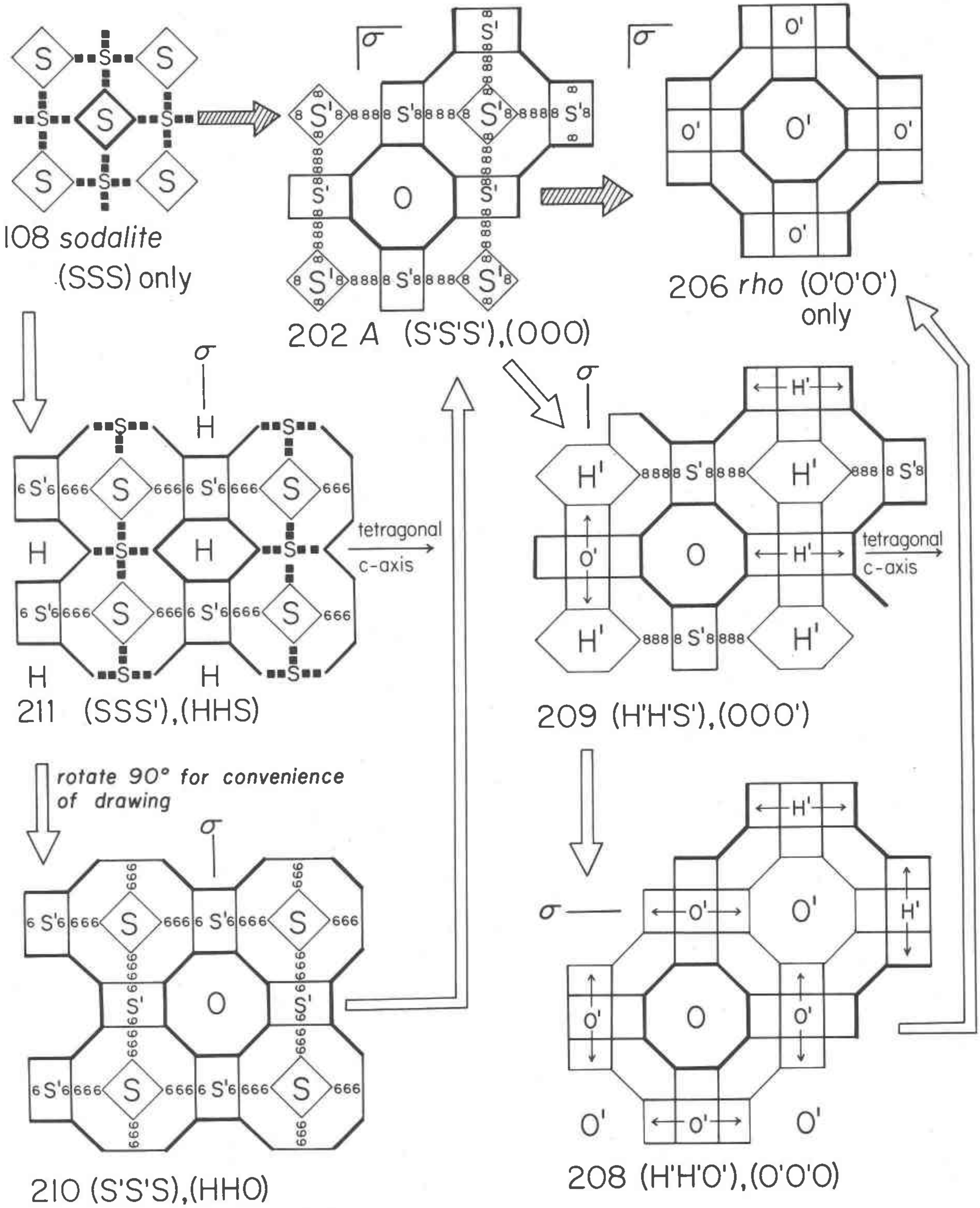

Fig. 3. 2D projections of three Archimedean and four near-Archimedean nets. Three symmetrical σ-operations (hatched arrow) convert net 108 (sodalite) to net 202(A), and three more operations yield net 206 (rho). The truncated-octahedral cage of sodalite has square 4-rings (S and squares) perpendicular to cubic axes, and these transform to the TCO cage with attached octagonal prisms (O′) in the rho net. There are two cages in the A net: a truncated cuboctahedron with octagonal faces (O and 88888), and a truncated octahedron with attached cubes (S′). One σ-operation converts 108 into 211 (open arrow) which is viewed perpendicular to the tetragonal *c*-axis; one cage has two hexagons (H and 66666) and a square in cubic directions, and the other has two S and one S′. Each S′ is viewed down a diad axis, and it overlaps with a vertical hexagon. Net 210 is obtained from 211 by a further σ-operation, and is viewed down the tetrad axis. In nets 208 and 209, H′ and O′ overlap, but only one symbol is listed at each place to avoid confusion. Net 208 is viewed down a tetrad axis.

Table 6. Enumeration of σ-related nets

Position(s) of operator(s)	Labels for net	
3	211(δ)	Only one choice for one operator; position 3 chosen because of tetragonal symmetry.
1,4	214(θ)	Only one choice for two parallel operators; net has isometric symmetry, and 1,4 = 2,5 = 3,6.
1,2	210(γ)	Only one choice for two non-parallel operators in same triplet; = 1,3 = 2,3 = 4,5 = 4,6 = 5,6.
1,6	215(λ)	Only one choice for two non-parallel operators in different triplets; = 1,6 = 2,4 = 2,6 = 3,4 = 3,5.
[1,2,3]	[202(A)]	Only one choice for three operators from same triplet = 4,5,6; Archimedean net.
1,2,6	213(η)	Three non-parallel operators, two from one triplet; = 1,3,5 = 2,3,4.
1,3,6	212(ε)	Two parallel and one non-parallel; = 1,3,4 = 2,3,5 = 2,3,6 = 1,2,4 = 1,2,5.
1,2,3,6	209(β)	Three in one triplet, and one in the other; = 1,2,3,4 = 1,2,3,5 = 1,4,5,6 = 2,4,5,6 = 3,4,5,6.
1,2,4,5	216(μ)	Two pairs of parallel operators; = 2,3,5,6 = 1,3,4,6.
1,2,4,6	217(π)	Two parallel and two non-parallel operators.
1,2,3,4,5	208(α)	Five operators.

Acknowledgments

We wish to pay tribute to earlier workers, and especially to the late Donald W. Breck whose early death terminated a brilliant career in zeolite chemistry. The present paper is particularly suitable as a tribute because DWB pointed out to JVS in 1956 that the absorption properties of chabazite did not match the structure then in the literature; this lead to discovery of the structures of chabazite and gmelinite by Lesley Dent-Glasser and JVS. Furthermore DWB was a co-discoverer of the structure of zeolite A and the inventor of zeolite Y. He also discovered the lonsdaleite analog of the faujasite net.

We thank Irene Baltuska for typing and Union Carbide Corporation and the National Science Foundation (grant CHE 78-28659) for support. Helpful criticism was provided by H. Gies.

References

Andreini, A. (1907) The nets of regular and semi-regular polyhedra and corresponding correlative nets. Societa Italiano Delle Scienze, Memorie di Mathematica de Fisica, series 3, 14, 75–129.

Bariand, P., Cesbron, F. and Giraud, R. (1968) Une nouvelle espèce minerale: l'afghanite de Sar-e-Sang, Badakhshan, Afghanistan. Comparaison avec les mineraux du groupe de la cancrinite. Bulletin de la Société francaise de Minéralogie et de Cristallographie, 91, 34–42.

Barrer, R. M. and Kerr, I. S. (1959) Intracrystalline channels in levynite and some related zeolites. Transactions Faraday Society, 55, 1915–1923.

Barth, T. F. W. (1932) The structures of the minerals of the sodalite family. Zeitschrift für Kristallographie, 83, 405–414.

Bennett, J. M. and Gard, J. A. (1967) Non-identity of zeolites erionite and offretite. Nature, 214, 1005.

Bergerhoff, G., Baur, W. H. and Nowacki, W. (1958) The crystal structure of faujasite. Neues Jahrbuch für Mineralogie, Monatshefte, 193–200.

Brown, W. L. and Cesbron, F. (1973) Sur les surstructures des cancrinites. Academie Sciences Paris Comptes Rendus, Séries D, 276, 1–4.

Danø, M. (1966) The crystal structure of tugtupite—a new mineral, $Na_8Al_2Be_2Si_8O_{24}(Cl,S)_2$. Acta Crystallographica, 20, 812–816.

Dent, L. S. and Smith, J. V. (1958) Crystal structure of chabazite, a molecular sieve. Nature, 181, 1794–1796.

Fischer, K. (1966) Untersuchung der Kristallstruktur von Gmelinit. Neues Jahrbuch für Mineralogie. Monatshefte, 1–13.

Foit, F. F., Jr., Peacor, D. R. and Heinrich, E. W. (1973) Cancrinite with a new superstructure from Bancroft, Ontario. Canadian Mineralogist, 11, 940–951.

Gard, J. A. and Tait, J. M. (1971) Structural studies on erionite and offretite. Advances in Chemistry Series, 101, 17–236.

Gard, J. A. and Tait, J. M. (1972) The crystal structure of the zeolite offretite, $K_{1.1}Ca_{1.1}Mg_{0.7}[Si_{12.8}Al_{5.2}O_{36}].-15 \cdot 2H_2O$. Acta Crystallographica, B28, 825–834.

Gramlich, V. and Meier, W. M. (1971) A crystal structure of hydrated NaA: A detailed refinement of a pseudosymmetric zeolite structure. Zeitschrift für Kristallographie, 133, 134–149.

Groner, M. and Meier, W. M. (1979) Reference in Meier and Olson (1978) to a forthcoming publication.

Holloway, W. M., Jr., Giordano, T. J. and Peacor, D. R. (1972) Refinement of the crystal structure of helvite, $Mn_4(BeSiO_4)_3S$. Acta Crystallographica, B28, 114–117.

Jarchow, O. (1965) Atomanordnung und Strukturverfeinerung von Cancrinite. Zeitschrift für Kristallographie, 122, 407–422.

Kawahara, A. and Curien, H. (1969) La structure cristalline de l'érionite. Bulletin de la Société francaise Minéralogie et de Crystallographie, 92, 250–256.

Kokotailo, G. T. and Lawton, S. L. (1964) Possible structures related to gmelinite. Nature, 203, 621–623.

Kokotailo, G. T. and Ciric, J. (1971) Synthesis and structural features of zeolite ZSM-3. Advances in Chemistry Series, 101, 109–121.

Kokotailo, G. T., Sawruk, S. and Lawton, S. L. (1972) Direct observation of stacking faults in the zeolite erionite. American Mineralogist, 57, 439–444.

Meier, W. M. and Kokotailo, G. T. (1965) The crystal structure of synthetic zeolite ZK-5. Zeitschift für Kristallographie, 121, 211–219.

Meier, W. M. and Olson, D. H. (1978) Atlas of Zeolite Structure Types. Polycrystal Book Service, Pittsburgh, Pa.

Merlino, S. and Mellini, M. (1976) Crystal structures of cancrinite-like minerals. Zeolite '76 Program and Abstracts, Tucson, Arizona, Meeting, p. 47.

Merlino, S. and Orlandi, P. (1977) Liottite, a new mineral in the cancrinite-davyne group. American Mineralogist, 62, 321–326.

Merlino, S. and Orlandi, P. (1977) Franzinite, a new mineral phase from Pitigliano (Italy). Neues Jahrbuch für Mineralogie Monatshefte, no. 4, 163–167.

Merlino, S., Galli, E. and Alberti, A. (1975) The crystal structure of levyne. Tschermaks Mineralogische und Petrographische Mitteilungen, 22, 117–129.

Moore, P. B. and Smith, J. V. (1964) Archimedean polyhedra as the basis of tetrahedrally-coordinated frameworks. Mineralogical Magazine, 33, 1008–1014. Erratum (1967) 36, 144.

Reed, T. B. and Breck, D. W. (1956) Crystalline zeolites II. Crystal structure of synthetic zeolite Type A. Journal of the American Chemical Society, 78, 5972–5977.

Rinaldi, R. (1976) Crystal chemistry and structural epitaxy of offretite-erionite from Sasbach, Kaiserstuhl. Neues Jahrbuch für Mineralogie Monatshefte, no. 4, 145–156.

Rinaldi, R. and Wenk, H.-R. (1979) Stacking variations in cancrinite minerals. Acta Crystllographica, A35, 825–828.

Robson, H. E., Shoemaker, D. P., Ogilvie, R. A. and Manor, P. C. (1973) Synthesis and crystal structure of zeolite Rho—A new zeolite related to Linde Type A. Advances in Chemistry Series, 121, 106–115.

Sahl, K. (1980) Refinement of the crystal structure of bicchulite, $Ca_2[Al_2SiO_6](OH)_2$. Zeitschrift für Kristallographie, 152, 13–21.

Sheppard, R. A., Gude, A. J. 3rd, Desborough, G. A. and White, J. S. Jr. (1974) Levyne-offretite intergrowths from basalt near Beech Creek, Grant County, Oregon. American Mineralogist, 59, 837–842.

Shoemaker, D. P., Robson, H. E. and Broussard, L. (1973) The "sigma transformation" interrelating certain known and hypothetical zeolite structures. Molecular Sieves (edited J. B. Uytterhoeven), Leuven University Press, Leuven, pp. 138–143.

Sieber, W. and Meier, W. M. (1974) Formation and properties of Losod, a new sodium zeolite. Helvetica Chimica Acta, 57, 1533–1540.

Smith, J. V. (1978) Enumeration of 4-connected 3-dimensional nets and classification of framework silicates, II. Perpendicular and near-perpendicular linkages from 4.8^2, 3.12^2 and 4.6.12 nets. American Mineralogist, 63, 960–969.

Smith, J. V. (1979) Enumeration of 4-connected 3-dimensional nets and classification of framework silicates, III. Combination of helix, and zigzag, crankshaft and saw chains with simple 2D nets. American Mineralogist, 64, 551–562.

Staples, L. W. and Gard, J. A. (1959) The fibrous zeolite erionite: its occurrence, unit cell, and structure. Mineralogical Magazine, 32, 261–281.

Taylor, D. (1967) The sodalite group of minerals. Contributions to Mineralogy and Petrology, 16, 172–188.

Wells, A. F. (1975) Structural Inorganic Chemistry, 4th edition, Clarendon Press, Oxford.

Wells, A. F. (1977) Three-dimensional Nets and Polyhedra, Wiley, New York.

Manuscript received, December 22, 1980; accepted for publication, March 10, 1981.